

SUPPLEMENTARY INFORMATION

RNA cytometry of single-cells using semi-permeable microcapsules

Greta Leonavičienė and Linas Mažutis

Institute of Biotechnology, Life Sciences Centre, Vilnius University, 7 Sauletekio av., Vilnius, Lithuania

Supplementary Tables

Supplementary Table S1. DNA primer sequences.

Name	Sequence (5'-3')	Product length
555-YAP-forward	Alexa Fluor 555-CCCTCGTTTTGCCATGAACC	584 bp
YAP-reverse	CCAGTGTTCCAAGGTCCACA	
488-PTPRC -forward	Alexa Fluor 488-ACATTGCTGCACAAGGTCCCAG	532 bp
PTPRC -reverse	AACCATCAGGCATCTCTGTGCGC	
647-ACTB-forward	Alexa Fluor 647-ATTCTATGTGGGCGACGA	607 bp
ACTB-reverse	AATGGTGATGACCTGGCCG	
647-B2M-forward	Alexa Fluor 647-AGCAGCATCATGGAGGTTTGA	513 bp
B2M-reverse	CCAGATTAACCACAACCATGCC	
647-TBP-forward	Alexa Fluor 647-GCGCAAGGGTTTCTGGTTTG	539 bp
TBP-reverse	TTTGCAGCTGCGGTACAATC	
555-PML-RARA-forward	Alexa Fluor 555-AGCGCGACTACGAGGAGAT	688 bp
PML-RARA-reverse	CTGCTGCTCTGGGTCTCAAT	
546-BCR-ABL-forward	Alexa Fluor 546-GAAGTGTTCAGAAGCTTCTCC	417 bp
BCR-ABL-reverse	GTTTGGGCTTCACACCATTC	
DNA primer sequences used for qPCR		
YAP-forward	CCCTCGTTTTGCCATGAACC	584 bp
YAP-reverse	CCAGTGTTCCAAGGTCCACA	
PTPRC -forward	ACATTGCTGCACAAGGTCCCAG	532 bp
PTPRC -reverse	AACCATCAGGCATCTCTGTGCGC	
ACTB-forward	ATTCTATGTGGGCGACGA	607 bp
ACTB-reverse	AATGGTGATGACCTGGCCG	
B2M-forward	AGCAGCATCATGGAGGTTTGA	513 bp
B2M-reverse	CCAGATTAACCACAACCATGCC	
TBP-forward	GCGCAAGGGTTTCTGGTTTG	539 bp
TBP-reverse	TTTGCAGCTGCGGTACAATC	
PML-RARA-forward	AGCGCGACTACGAGGAGAT	688 bp
PML-RARA-reverse	CTGCTGCTCTGGGTCTCAAT	
BCR-ABL-forward	GAAGTGTTCAGAAGCTTCTCC	417 bp
BCR-ABL-reverse	GTTTGGGCTTCACACCATTC	

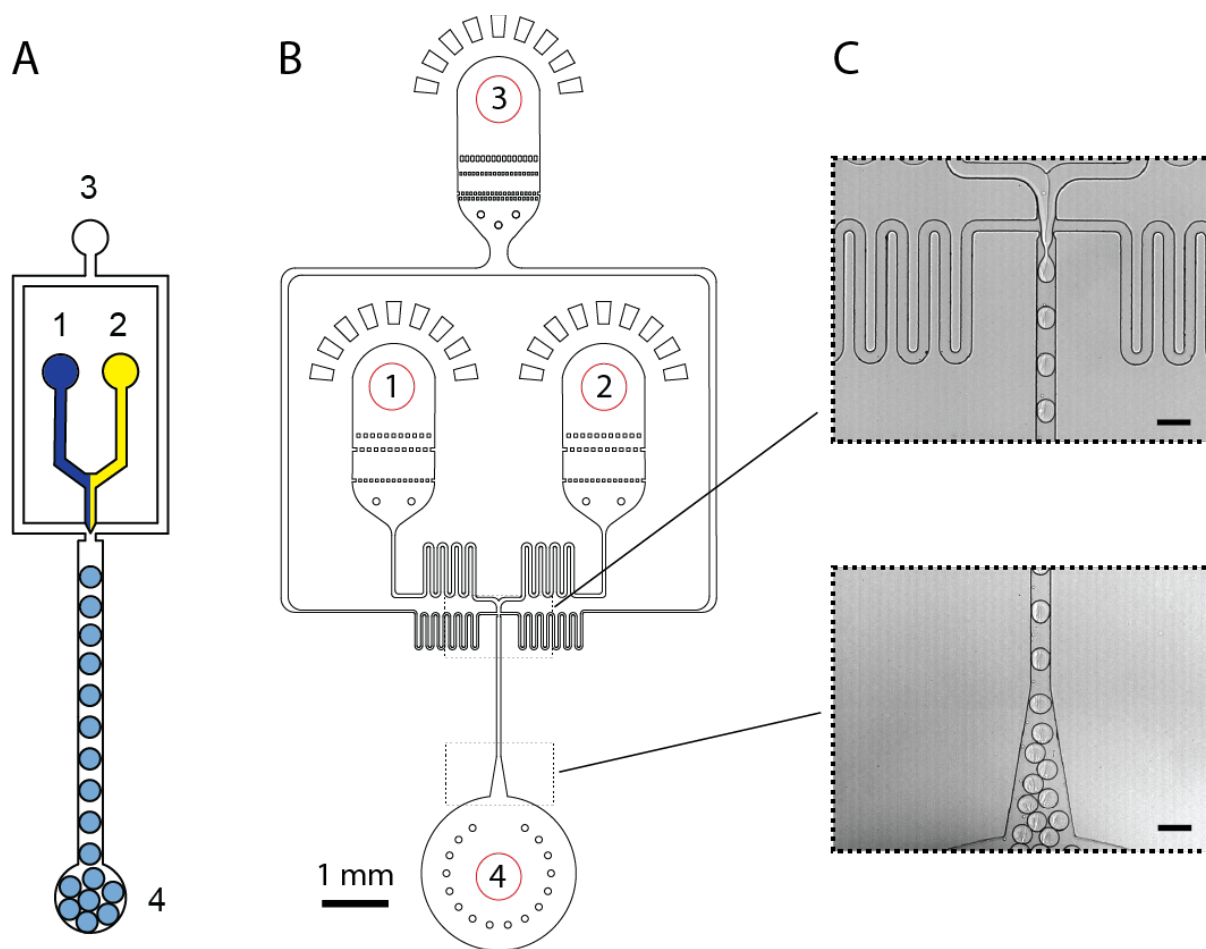
Supplementary Table S2. The Ct values of the marker genes determined by bulk RT-qPCR.

Sample	The Ct values* of marker genes						
	ACTB	B2M	TBP	PTPRC	YAP	PML-RARA	BCR-ABL
K-562	16.74 ± 0.13	18.07 ± 0.03	22.80 ± 0.02	22.95 ± 0.03	No signal	Not tested	21.76 ± 0.06
HEK293	15.58 ± 0.08	18.15 ± 0.11	21.54 ± 0.11	34.01 ± 0.34	21.26 ± 0.14	Not tested	Not tested
NB-4	15.16 ± 0.19	16.27 ± 0.06	22.87 ± 0.10	21.58 ± 0.03	Not tested	29.26 ± 0.23	No signal
PBMC	20.47 ± 0.07	19.00 ± 0.05	29.62 ± 0.22	22.51 ± 0.13	Not tested	No signal	Not tested
NTC	No signal	No signal	No signal	No signal	No signal	No signal	No signal

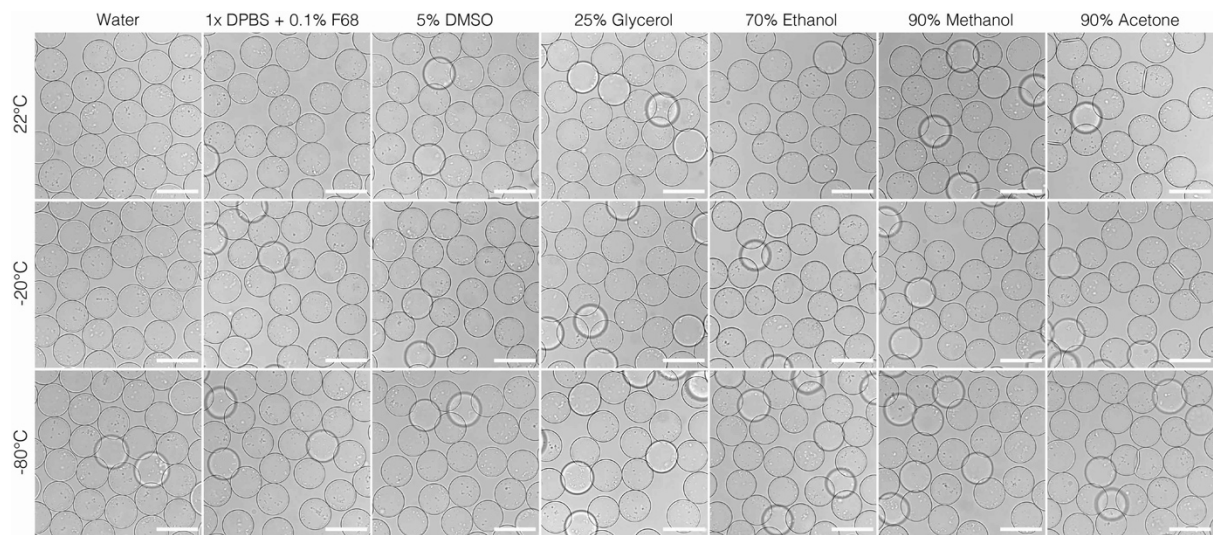
* The Ct values were determined by real-time qPCR on QuantStudio 1 instrument using 40 ng/μl of total RNA extracted from K-562, HEK293 and NB-4 cells, and 5 ng/μl of total RNA extracted from PBMCs (ATCC). The primer pairs used for qPCR are listed in Supplementary Table S1. The values represent the mean and standard deviation from three technical replicates.

Supplementary Table S3. Comparative analysis of the multiplex single cell RT-PCR results using flow cytometry and epifluorescence microscopy.

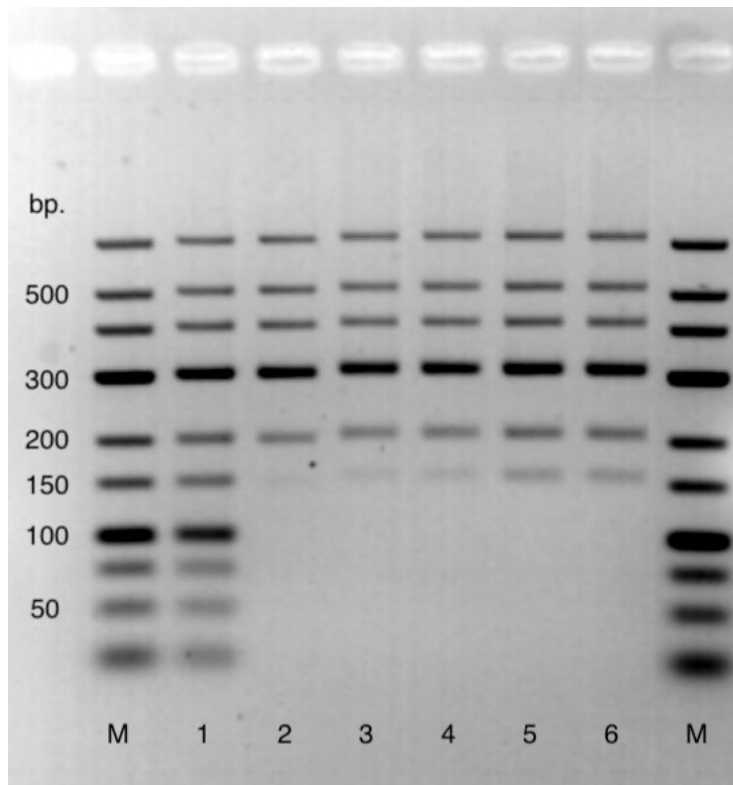
Sample ID	Total counts	ACTB positive	YAP positive	YAP & ACTB positive	PTPRC positive	PTPRC & ACTB positive	YAP & PTPTC Positive	YAP & PTPTC & ACTB positive
Microscopy analysis								
K-562	2822	285 (10.1%)	3 (0.11%)	3 (0.11%)	90 (3.19%)	90 (3.19%)	2 (0.07%)	2 (0.07%)
HEK293	2128	272 (12.78%)	103 (4.84%)	102 (4.79%)	0 (0.0%)	0 (0.0%)	0 (0.0%)	0 (0.0%)
K-562 & HEK293	2006	361 (18.0%)	69 (3.44%)	68 (3.39%)	36 (1.79%)	36 (1.79%)	3 (0.15%)	3 (0.15%)
FACS analysis								
K-562	23628	2565 (10.86%)	84 (0.36%)	18 (0.08%)	858 (3.63%)	850 (3.60%)	1 (<0.01%)	1 (<0.01%)
HEK293	19574	2800 (14.30%)	1069 (5.46%)	1011 (5.17%)	1 (<0.01%)	1 (<0.01%)	6 (0.03%)	6 (0.03%)
K-562 & HEK293	31061	5881 (18.93%)	940 (3.03%)	863 (2.78%)	524 (1.69%)	516 (1.66%)	6 (0.02%)	5 (0.02%)



Supplementary Figure S1. Design of the microfluidics device and its operation. **A)** Operation of the microfluidics device. The microfluidics device contains two aqueous inlets (#1 and #2) for injecting core forming solution and shell forming solution, one inlet for the carrier oil (#3) and one outlet for collecting the droplets (#4). The water-in-oil droplets are generated at a flow-focusing junction, collected at the collection outlet in the form of emulsion and are converted to microcapsules using a two-step polymerization process as detailed in Materials and Methods section. **B)** Design of the microfluidics device. Scale bar 1 mm. **C)** Digital micrographs showing droplet generation and collection. Scale bars, 100 μm .



Supplementary Figure S2. Evaluation of microcapsule stability. Bright field microscopy images of the microcapsules in different solvents at room temperature (top row), after freezing at -20 °C for 16 hours (middle row), and after freezing at -80 °C for 16 hours (bottom row). Scales bars, 100 μm .



Supplementary Figure S3. Double stranded DNA retention in microcapsules at different temperatures. Agarose gel showing DNA retention in microcapsules after incubation for 30 minutes at different temperatures ranging from 4 to 70 °C. The GeneRuler Low Range DNA Ladder (Thermo Fischer Scientific, SM1191) was used to evaluate the size of retained DNA molecules in microcapsules. After a 30-minute incubation at a given temperature, the microcapsules were broken and the collected DNA was loaded on agarose gel for DNA electrophoresis.

M – GeneRuler Low Range DNA Ladder.

1 – DNA retention in water-in-oil emulsion.

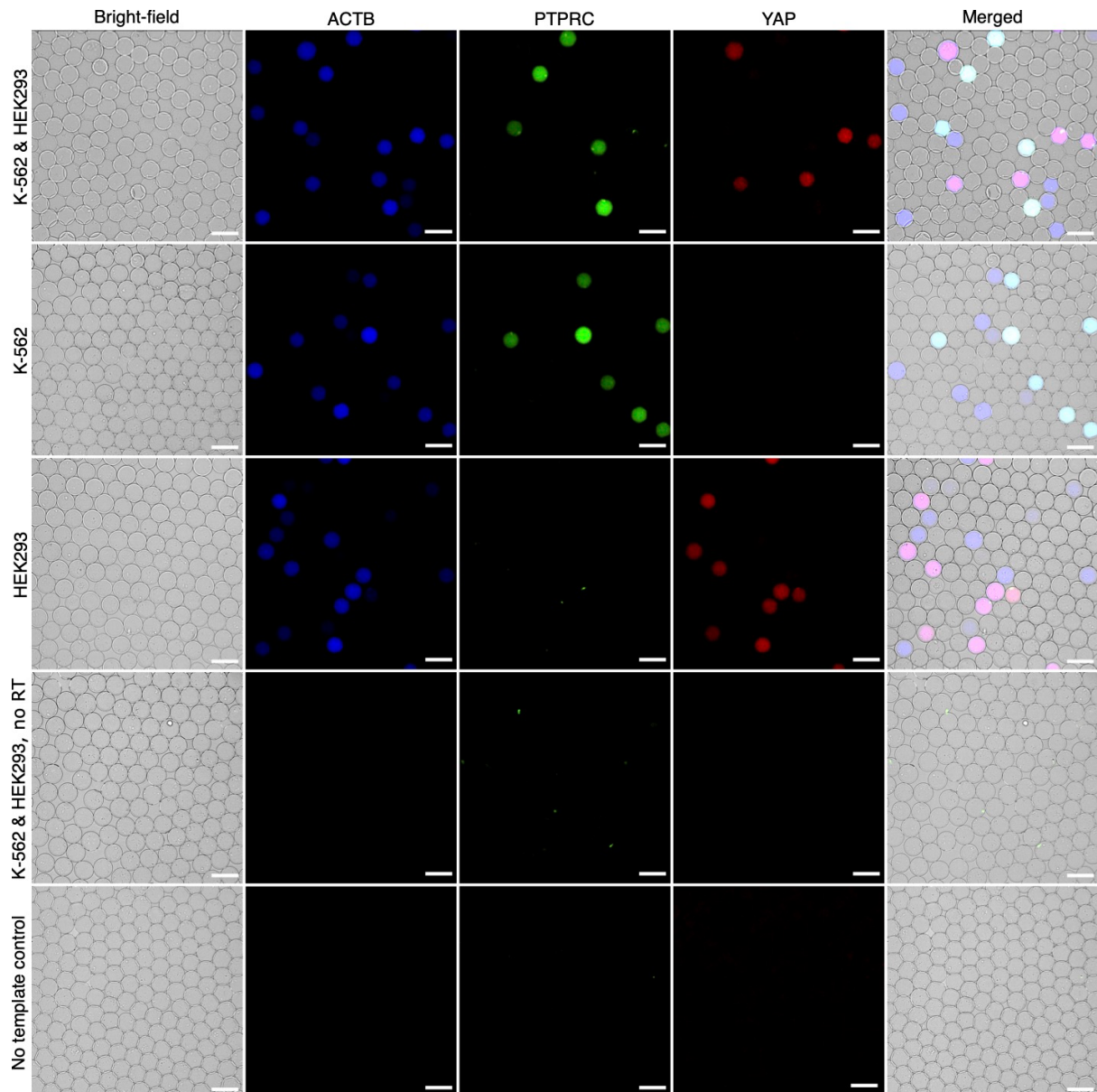
2 – DNA retention in microcapsules after physical gelation and incubation at 4 °C for 30 min.

3 – DNA retention in microcapsules after chemical cross-linking and incubation at 4 °C for 30 min.

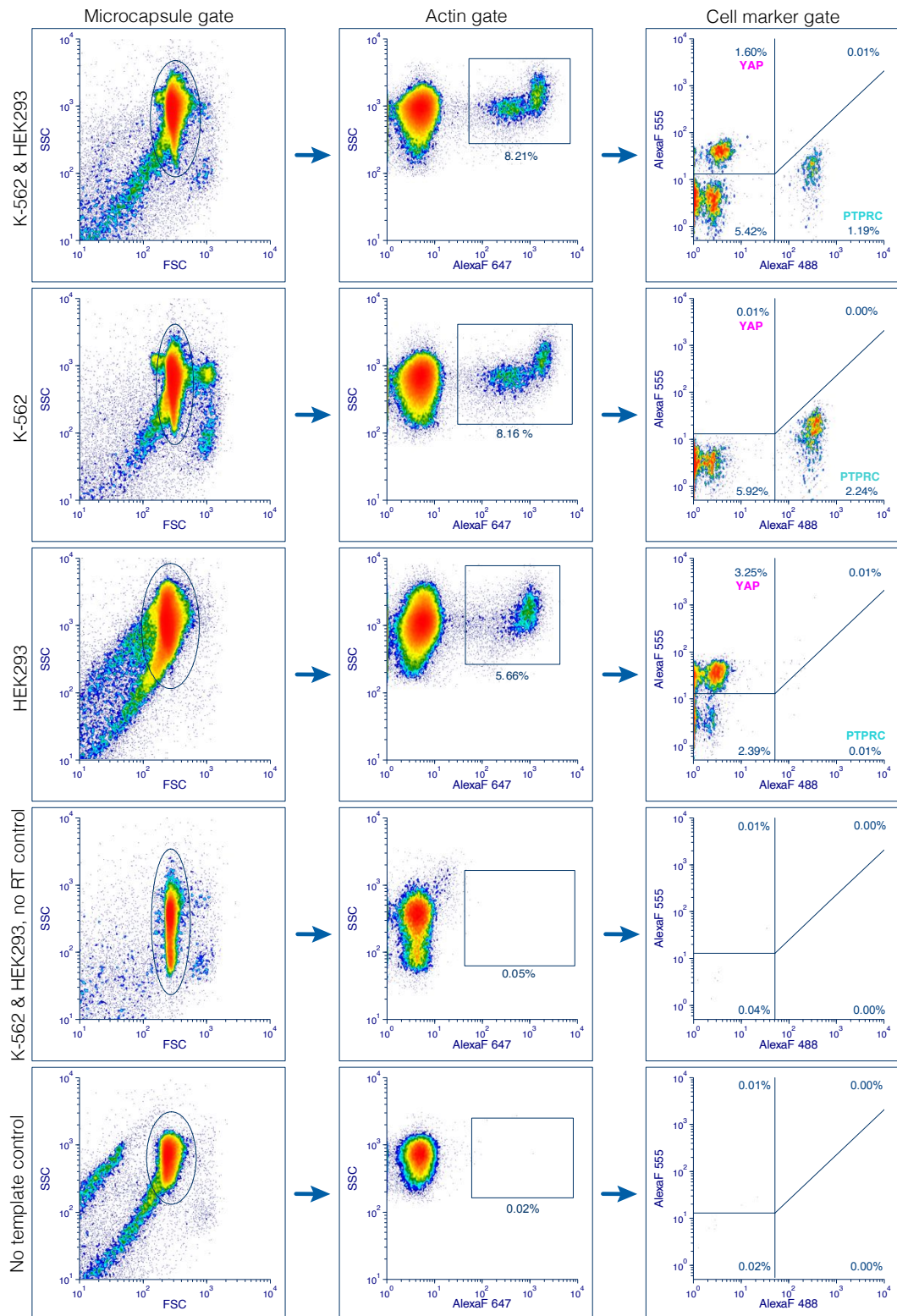
4 – DNA retention in microcapsules after chemical cross-linking and incubation at 22 °C for 30 min.

5 – DNA retention in microcapsules after chemical cross-linking and incubation at 50 °C for 30 min.

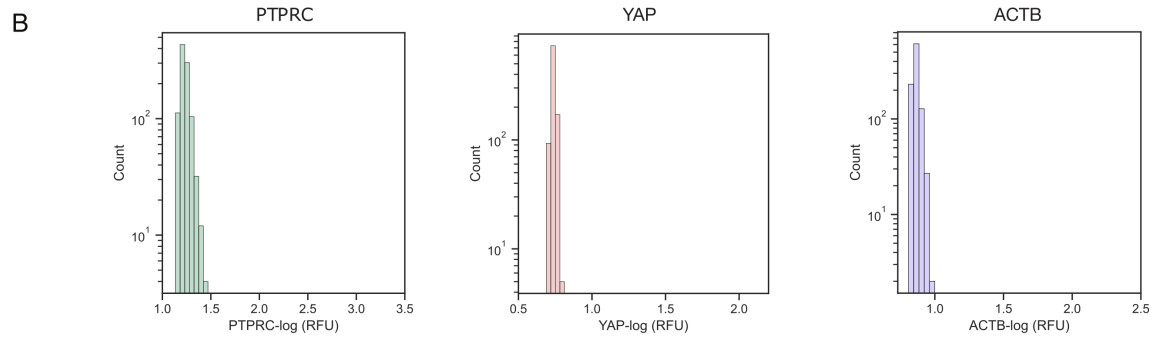
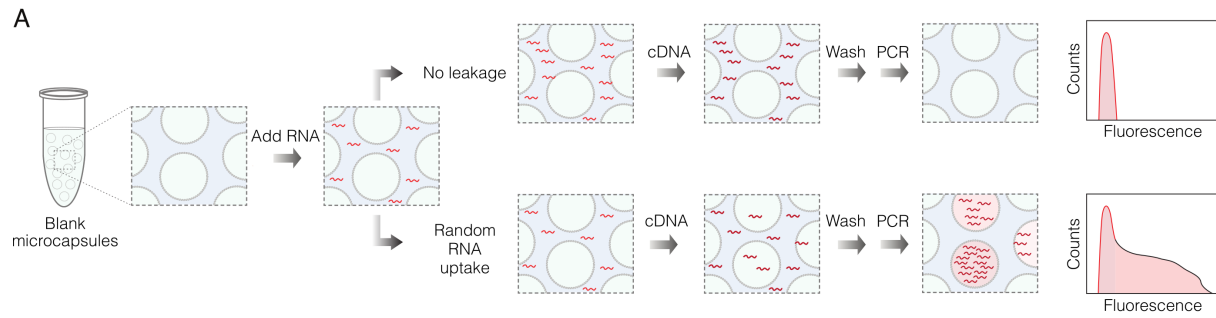
6 – DNA retention in microcapsules after chemical cross-linking and incubation at 70 °C for 30 min.



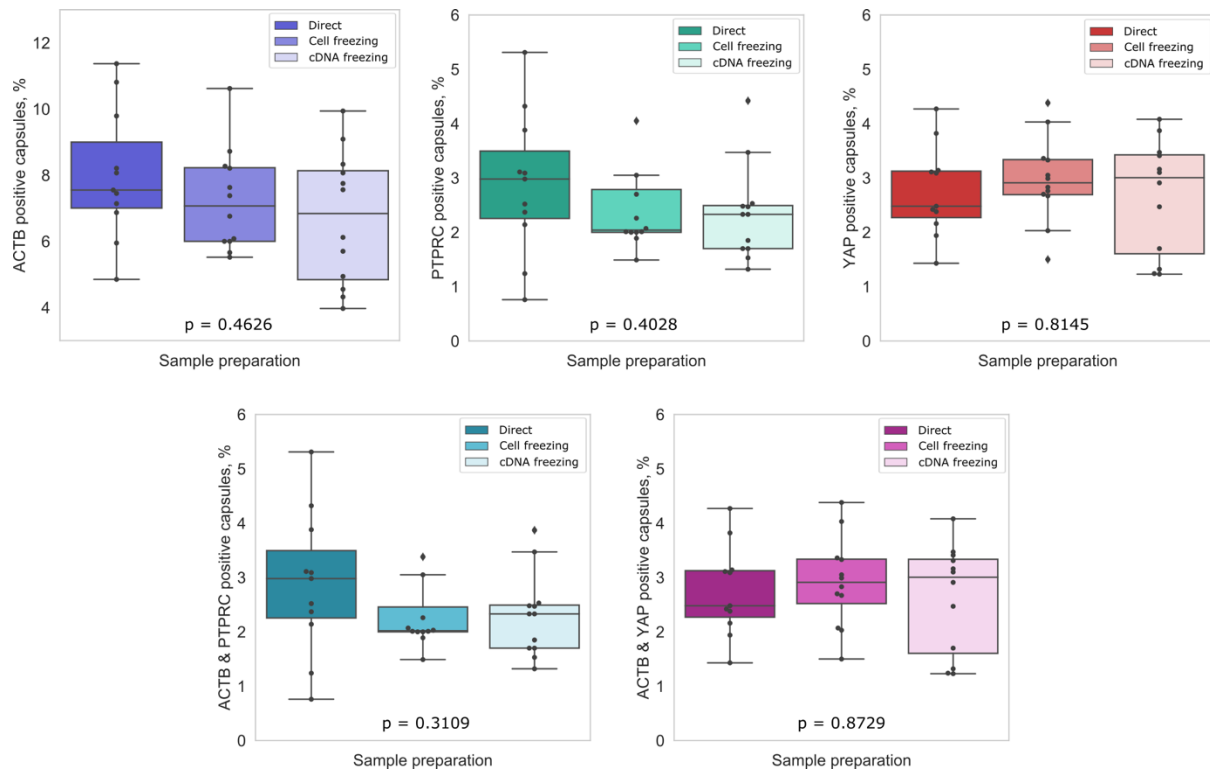
Supplementary Figure S4. Microcapsule-based single-cell RT-PCR. Digital microscopy images of microcapsules following a multiplex RT-PCR assay prepared with different biological samples. After cell encapsulation and prior to the reverse transcription step, the microcapsules were treated with DNase I enzyme to deplete the gDNA. From top to bottom microcapsules comprised: a mixture of K-562 and HEK293 cells (1st row), K-562 cells alone (2nd row), HEK293 cells alone (3rd row), no RT enzyme control (4th row), and no template control (5th row). The digital images from left to right indicate: bright field, Alexa Fluor 647 fluorescence for ACTB marker (blue), Alexa Fluor 488 fluorescence for PTPRC marker (green), Alexa Fluor 555 fluorescence for YAP marker (red) and merged image where bright field and fluorescence photographs are superimposed. Scale bars, 100 μm .



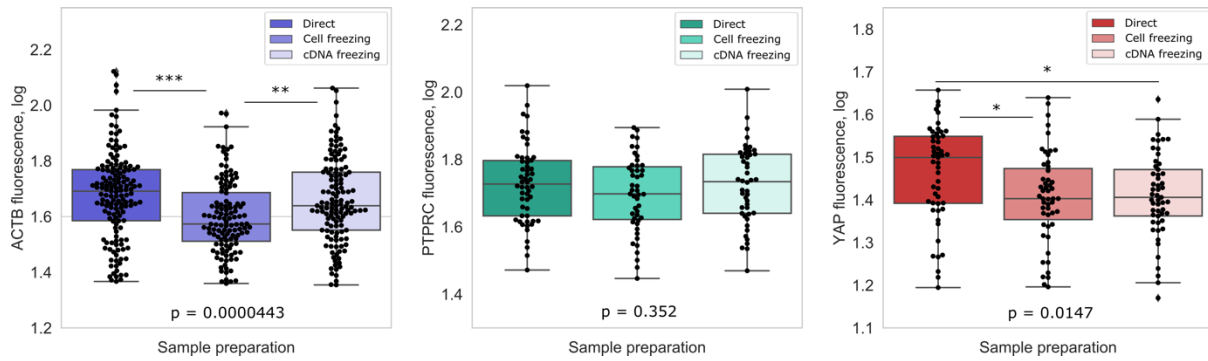
Supplementary Figure S5. Flow cytometry of microcapsules following single-cell RT-PCR. The flow cytometry analysis of microcapsules prepared with a mixture of K-562 and HEK293 cells (top row), K-562 cells (2nd row), HEK293 cells (3rd row), no RT enzyme control (4th row) and no template control (5th row). The microcapsules were first gated based on forward and side scatter (Microcapsule gate), expression of ACTB marker (Actin gate) and then the expression of PTPRC and YAP markers was recorded (Cell marker gate). Due to the emission overlap of Alexa Fluor 488 and Alexa Fluor 555 dyes and imperfect compensation process, the PTPRC-positive population showed an increased fluorescence in Alexa Fluor 555 channel. The percentages indicate the total events ($n \sim 100,000$).



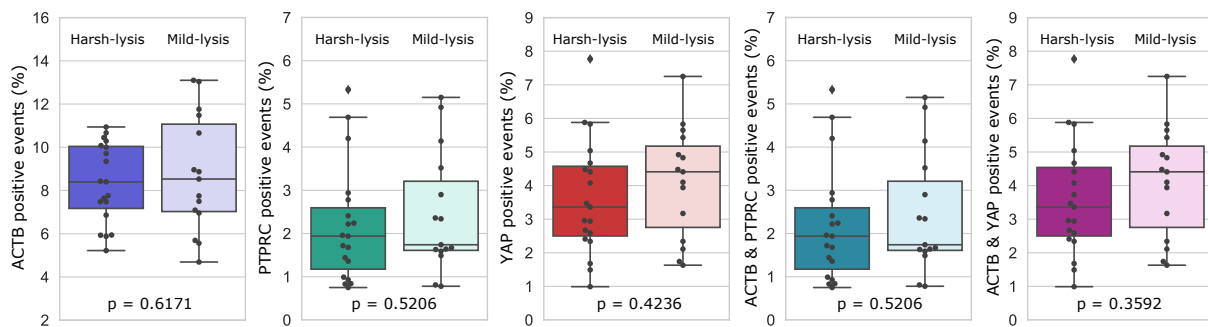
Supplementary Figure S6. RNA and cDNA leakage test. A) Experimental scheme. Purified total RNA (2 μg) from a mixture of HEK293:K-562 cells is added to the RT reaction mixture ($V = 200 \mu\text{l}$) supplemented with $\sim 200,000$ blank (empty) microcapsules. After cDNA synthesis, the microcapsules were washed to remove unretained RNA and cDNA molecules, and transferred to PCR reaction mixture to amplify YAP, PTPRC and ACTB targets. In the presence of RNA or cDNA uptake the microcapsules will show increased fluorescence, in the absence of leakage the microcapsules will remain blank (non-fluorescent). **B)** The fluorescence histograms for PTPRC, YAP and ACTB markers were constructed by measuring the fluorescence of post-RT-PCR microcapsules ($n \sim 1000$) following the experiments scheme indicated in panel A.



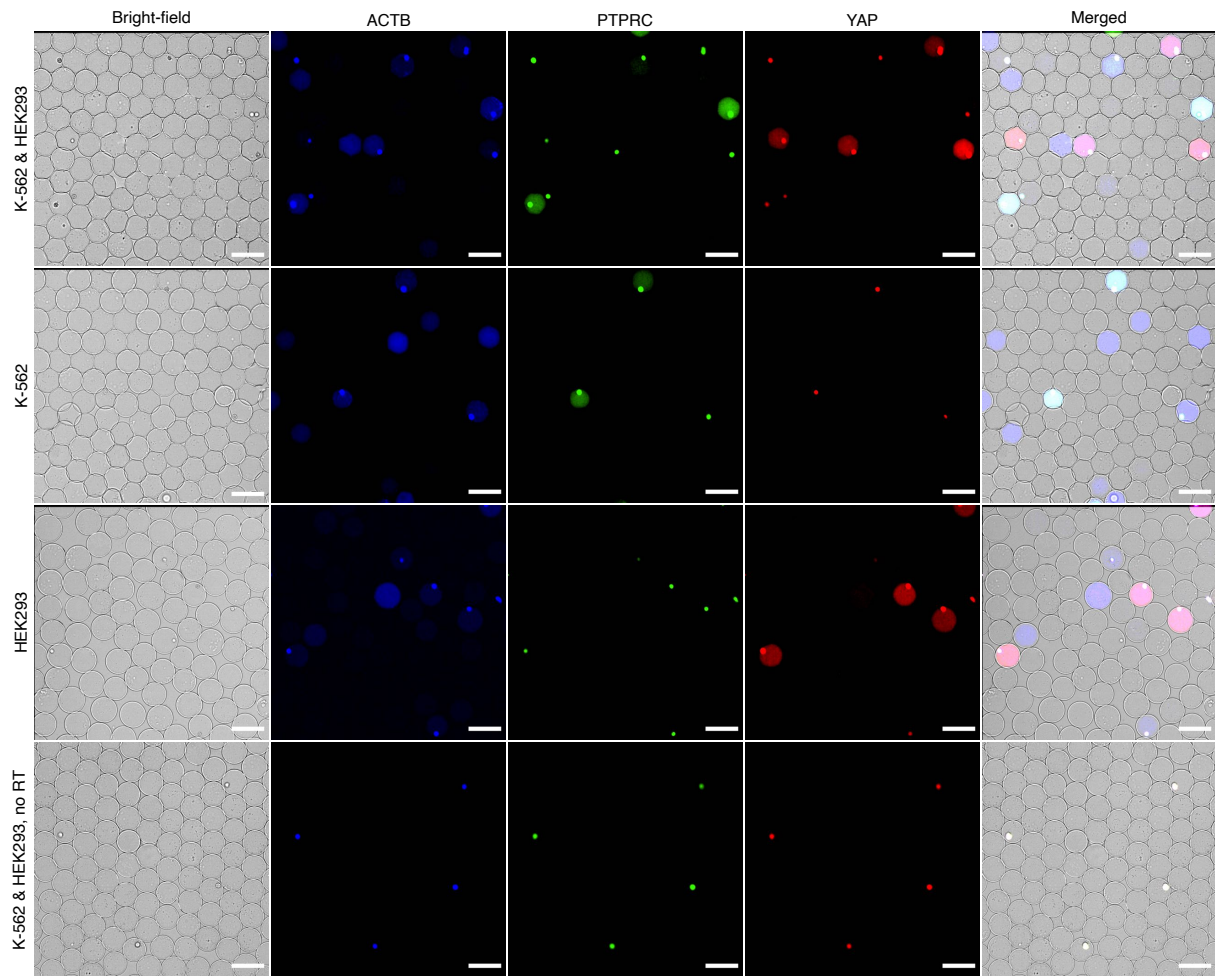
Supplementary Figure S7. Performance of multiplex scRT-PCR on live-cells, ethanol-preserved cells and ethanol-preserved cDNA samples. The boxplots representing the distribution of positive microcapsules for ACTB, PTPRC, YAP, ACTB & PTPRC and ACTB & YAP markers obtained following three different sample preparation workflows. To begin with the microcapsules carrying a mixture of K-562 and HEK293 cells were divided into three parts. The first part (Direct workflow) was processed under the harsh-lysis conditions followed by gDNA depletion as detailed in Materials and Methods section. The second part (Cell freezing workflow) was dispersed in 70% (v/v) ethanol to fix the encapsulated cells, transferred to -20 °C for 20-24 hours, thawed and then subjected to harsh-lysis and gDNA depletion. The third part (cDNA freezing workflow) was treated under the harsh-lysis and gDNA depletion conditions, subjected to cDNA synthesis and then frozen at -20 °C in 70% (v/v) ethanol. All three workflows were subjected to the same RT and PCR conditions. The p values were calculated applying nonparametric Kruskal-Wallis test. All p values were higher than 0.05, which indicates statistically insignificant differences between sample processing techniques.



Supplementary Figure S8. Fluorescence intensity of multiplex scRT-PCR assay on live-cells, alcohol-preserved cells and alcohol-preserved nucleic acid material. The measured fluorescence intensities of ACTB (left), PTPRC (middle) and YAP (right) amplicons are plotted. Three different workflows were tested: direct workflow on live-cells (Direct), ethanol-fixation of cells and freezing at -20°C (Cell freezing) and cDNA preservation workflow on the cDNA material that was generated from live-cells in microcapsules, and then frozen at -20°C in 70% ethanol (cDNA freezing). One-way ANOVA showed there is no statistically significant difference in mean PTPRC fluorescence between different sample preparations ($p = 0.352$). However, statistically significant differences in mean fluorescence signal intensity were observed for ACTB ($p = 0.0000443$) and YAP ($p = 0.0147$). Pairwise comparison using Tukey post hoc test revealed that statistically significant differences in mean ACTB fluorescence intensity exist between direct workflow and cell freezing ($p < 0.001$) and cell freezing and cDNA freezing ($p = 0.0033$). Likewise, statistically significant differences in mean YAP fluorescence intensity were obtained between direct workflow and cell freezing ($p = 0.0254$) and direct workflow and cDNA freezing ($p = 0.0382$). In addition, the distribution normality was verified applying Lilliefors (Kolmogorov-Smirnov) normality test. Corresponding p values for ACTB, PTPRC and YAP fluorescence were 0.1118, 0.6766, 0.3761, which confirm a normal data distribution. The Levene's test for homogeneity of variance gave p values for ACTB, PTPRC and YAP fluorescence 0.2213, 0.9549 and 0.2439, respectively.

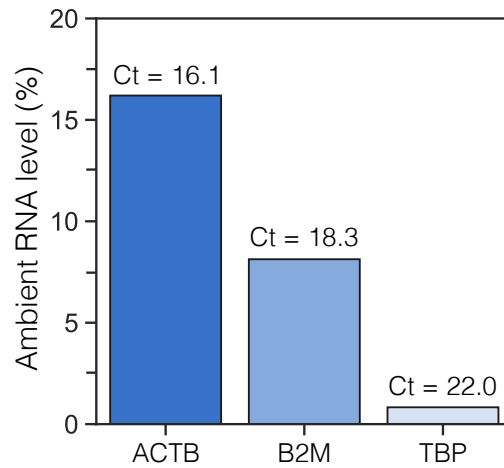


Supplementary Figure S9. Comparison of multiplex scRT-PCR output using mild- and harsh-lysis protocols. The boxplots represent the distribution of ACTB, PTPRC, YAP, ACTB & PTPRC and ACTB & YAP positive events in microcapsule-based RT-PCR assay following two cell lysis conditions. Under the harsh-lysis conditions the encapsulated cells were treated using GeneJET lysis buffer and DNase I as detailed in Materials and Methods section. Under the mild-lysis conditions the encapsulated cells were first fixed in ethanol and then lysed with non-ionic detergent Igepal CA-630 as detailed in Materials and Methods section. The p values were calculated by applying nonparametric Wilcoxon rank sum test. The p values were higher than 0.05, which indicates statistically insignificant differences between the mild- and harsh-lysis protocols.

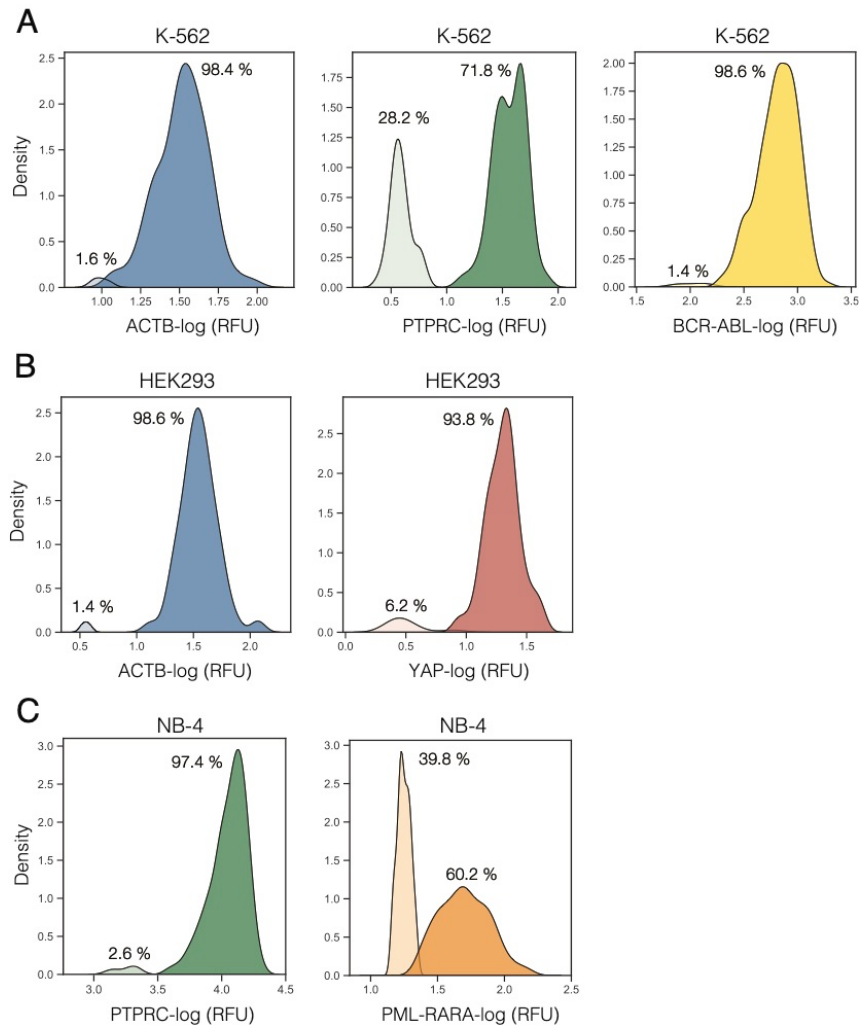


Supplementary Figure S10. Microcapsule-based single-cell RT-PCR following cell preservation.

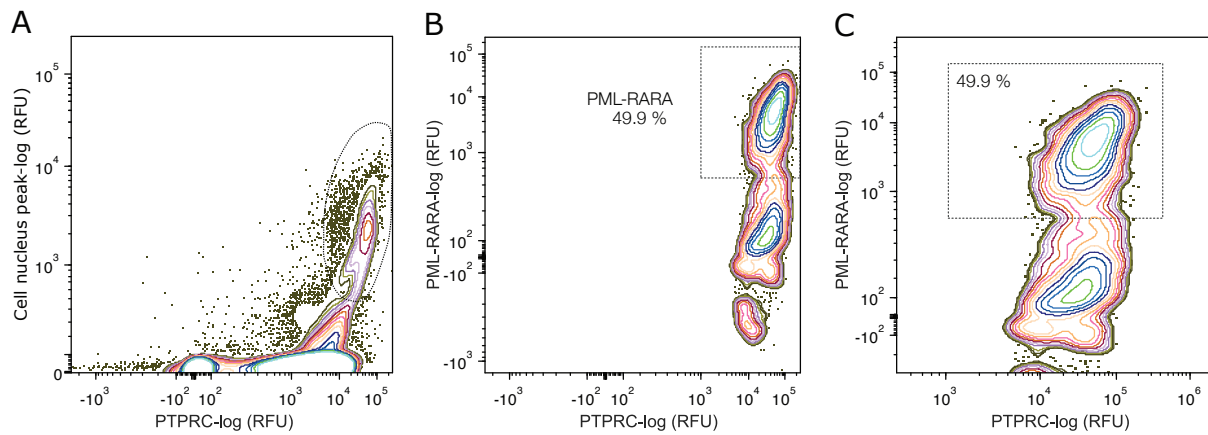
Digital microscopy images of microcapsules following a multiplex RT-PCR assay under conditions that preserve cell nucleus. The encapsulated cells were preserved in ice-cold ethanol and subjected to multiplex RT-PCR targeting ACTB (blue), PTPRC (green) and YAP (red). From top to bottom microcapsules comprised: a mixture of K-562 and HEK293 cells (1st row), K-562 cells alone (2nd row), HEK293 cells alone (3rd row), no RT enzyme control (4th row). The digital images from left to right indicate: bright field, Alexa Fluor 647 fluorescence for ACTB marker (blue), Alexa Fluor 488 fluorescence for PTPRC marker (green), Alexa Fluor 555 fluorescence for YAP marker (red) and merged image where bright field and fluorescence photographs are superimposed. Scale bars, 100 μm .



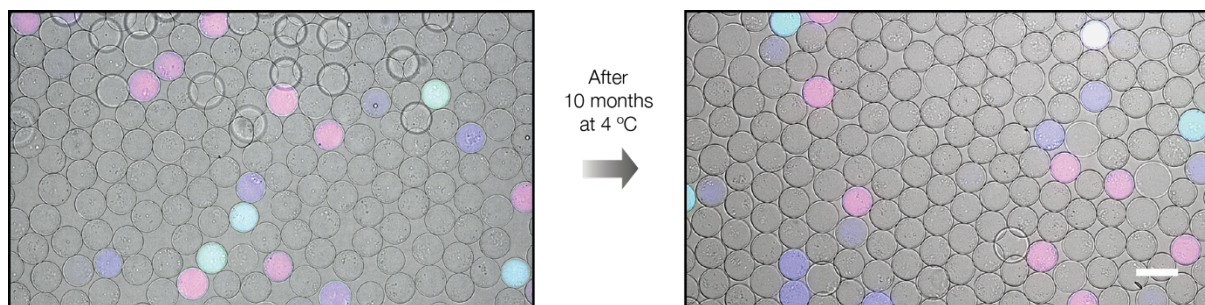
Supplementary Figure S11. The ambient RNA levels for different housekeeping genes in a mixture containing K-562 and HEK293 cells. The ambient RNA levels were determined by performing multiplex RT-PCR on a mixture of K-562 / HEK293 cells and recording the fraction of the cell-free microcapsules positive for a given housekeeping gene. The percentage on Y-axis is expressed as $y = \left(\frac{n_1}{n_1 + n_2}\right) \times 100\%$, where n_1 is cell-free microcapsules positive for a given housekeeping gene and n_2 is microcapsules carrying cells and are positive for a housekeeping gene. The average Ct values obtained from three independent bulk RT-qPCR experiments.



Supplementary Figure S12. Digital profiling of K-562, HEK293 and NB-4 cells for marker gene expression. The histograms represent the fluorescence distribution of microcapsule-based scRT-PCR readout for ACTB (blue), YAP (red), PTPRC (green), BCR-ABL (yellow) and PML-RAR α (orange) transcripts in individual cell lines. **A**) Digital profiling of K-562 cells for ACTB, PTPRC and BCR-ABL fusion expression. **B**) Digital profiling of HEK293 cells for ACTB and YAP expression. **C**) Digital profiling of NB-4 cells for PTPRC and PML-RAR α fusion expression.



Supplementary Figure S13. Gating strategy for analyzing PML-RAR α expression using FACS instrument. **A)** At first microcapsules are gated based on the fluorescence signal of cell nuclei (Y-axis) and ubiquitously expressed marker PTPRC (X-axis). **B)** The microcapsules with cells from panel A are then evaluated for co-expression of PML-RAR α and PTPRC, replotted in panel C, which is then reported in the main text (Figure 6).



Supplementary Figure S14. Single-cell RT-PCR amplicon retention in microcapsules over a period of 10 months. The mixture of K-562 of HEK293 cells was encapsulated in microcapsules, lysed and their gDNA digested with DNase I. Next, the microcapsules were subjected to reverse transcription using poly(dT) primers followed by multiplex PCR using fluorescently labelled primers (Supplementary Table S1) targeting cDNA molecules encoding PTPRC, YAP and ACTB markers. The PCR amplicons for PTPRC, YAP and ACTB markers, were 532, 584 and 607 bp. size, respectively. The post-RT-PCR microcapsules were imaged under epifluorescence microscope at day 1 (left) and 297 days later (right). During this period of time the microcapsules were stored at 4 °C in 10 mM Tris-HCl [pH 7.5], 0.1% Triton-X-100, 1 mM EDTA buffer. No significant fluorescence difference or change in occupancy was recorded between day-1 and day-297. At day-1, the percentage of ACTB, PTPRC and YAP positive microcapsules was 8.2% 1.9% and 3.7%, respectively. At day-297, the percentage of ACTB, PTPRC and YAP positive microcapsules remained nearly the same: 8.1%, 1.85% and 3.7%, respectively. Scale bar 100 μ m.